

Orientation of CRP-3 Core, Victoria Land Basin, Antarctica

R.D. JARRARD^{1*}, T.S. PAULSEN², & T.J. WILSON³

¹Dept. of Geology & Geophysics, 717 WBB, Univ. of Utah 135 S. 1460 East, Salt Lake City UT 84112-0111 - U.S.A.

²Dept. of Geology, University of Wisconsin, 800 Algoma Blvd., Oshkosh, WI 54901 - U.S.A.

³Dept. of Geological Sciences, Ohio State University 275 Mendenhall, 125 S. Oval Mall, Columbus OH 43210 - U.S.A.

Received 28 October 2000; accepted in revised form 22 February 2001

Abstract - CRP-3 cores were not orientated with respect to North during coring operations. However, borehole televiwer (BHTV) logging did obtain azimuthally orientated images of the borehole wall, and core processing included digital imaging of the outer surface of 85% of the cores. Images of many individual core segments can be digitally joined, or stitched, by rotating them to match the shapes of their adjoining surfaces and then closing the gap. By aligning features (fractures, bedding, and clasts) on stitched-core images with correlative features on orientated BHTV images, we reorientated 231 m of core, or 25% of the cored interval. We estimate that the orientation uncertainty is $\pm 10^\circ$ for entire stitched-core intervals, and $\pm 15^\circ$ for individual features such as a single fracture or palaeomagnetic sample. Reliability of core orientations was confirmed by comparing azimuths of bedding and fractures measured directly within these reorientated cores to those measured within orientated borehole televiwer images.



INTRODUCTION

The Cape Roberts Project (CRP) is an international drilling project whose aim is to reconstruct Neogene to Palaeogene palaeoclimate and the tectonic history of the Transantarctic Mountains and West Antarctic rift system by obtaining continuous cores and well logs from a site near Cape Roberts, Antarctica. Offshore Cape Roberts, tilting and erosion of strata have brought Miocene to Lower Oligocene sediments near the seafloor, under a thin veneer of Quaternary sediments. The three CRP boreholes penetrate successively older portions of a 1600 m composite stratigraphic sequence.

The third CRP drillhole, CRP-3, cored 821 m of Lower Oligocene and possibly Upper Eocene sedimentary rocks and 116 m of underlying Devonian sandstone (Cape Roberts Science Team, 2000). Drilling and coring occurred in two phases: HQ-size drill rod (6.1-cm core diameter) was employed for coring of the interval 3-346 mbsf, followed by NQ-size coring (4.5-cm core diameter) of the interval 346-939 mbsf. Average core recovery was 97%. The section consists primarily of sandstones and muddy sandstones; other lithologies include common thin conglomerate beds and less common sandy mudstones and diamicrites (Cape Roberts Science Team, 2000).

Cores from the three CRP drillholes were not orientated with respect to North during drilling. Many CRP-1 cores could be reorientated using palaeomagnetic techniques (Paulsen & Wilson, 1998), and many CRP-2/2A cores were reorientated (Paulsen

et al., 2000) based on borehole televiwer (BHTV) measurement of azimuths of petal center-line fractures (Moos et al., 2000). Our study applies an alternative technique to reorientate CRP-3 cores: alignment of features (fractures, bedding, or clasts) on core-scan images with correlative, orientated features on BHTV images.

METHODS

CORE DATA ACQUISITION AND PROCESSING

Essential first steps for core reorientation occurred during initial core processing at the drillsite. These steps included identification of core runs that could be fitted together by matching fractures across run breaks, refitting core across fracture breaks within core runs, and logging of all fractures where spinning of the core between drilling and entry into the core barrel had disrupted the continuity of the core. Systematic examination and logging of all core breaks then allowed us to partition the core into intact intervals which had undergone no internal rotations. Each of these intact intervals must be reorientated independently, since rotations between adjacent intervals may have occurred. In CRP-3 core, ~300 independent intact core intervals, ranging in length from 10 cm to 30.4 m, were logged. To date, our reorientation analysis has focussed on the longer intact core intervals and on intervals within heavily faulted zones.

*Corresponding author (jarrard@mail.mines.utah.edu)

Upon recovery and reconstruction of the core, red and blue scribe lines were drawn $\sim 180^\circ$ apart along the length of the core. Dip and dip azimuth of all core fractures were measured with reference to the “arbitrary north” defined by the red scribe line. The core was then cut into 1-m segments. For all segments of core with enough integrity to permit handling, we scanned the outer surface of the core using Corescan® equipment leased from DMT, Germany. The Corescan® obtains digital images by rotating the whole core on rollers. After scanning, the core was moved to the physical properties lab for analysis, split in half lengthwise at $\sim 90^\circ$ to the scribe lines, and finally the two resulting half-cores were placed into an archive-half box and a working-half box. As a consequence of this core processing procedure, it is possible to retroactively reorientate any core features (*e.g.*, bedding and fractures) or samples (*e.g.*, palaeomagnetic plugs) with respect to North if two conditions are fulfilled: orientation with respect to the red scribe is measured, and the core interval has been reorientated with respect to North.

In post-field processing, we selected 17 intact core intervals for “stitching”. Stitching is the process of digitally joining two or more whole-core images, using DMT Corelog® software. Using this software one can apply differential rotations to adjacent segments and merge the images into a single restored (pre-break) image. This digital stitching is more accurate than the manual refitting of core segments undertaken just before red scribing. Although the red scribe is positioned at the top left margin of each stitched-core image, downcore drift of the scribe away from the left margin occurs due to imprecise scribing. Stitched core image files were imported into WellCAD® software at a vertical resolution of 1 mm. After import, image files were converted from color to gray levels, then displayed using a false-color spectrum encompassing a short amplitude range, to enhance subtle variations in brightness. We assumed a uniform core diameter of 61 mm for HQ cores and 45 mm for NQ cores.

BHTV DATA ACQUISITION AND PROCESSING

Borehole televiewer (BHTV) well logging was undertaken during three separate phases of CRP-3 drilling. The BHTV is an acoustic instrument that provides an image of surface reflectivity of the wall of a fluid-filled borehole (Zemanek et al., 1970). An acoustic transducer in the tool fires a sound pulse that travels through the borehole fluid, bounces off the borehole wall, and returns to the transducer. As the tool is pulled up the borehole, the transducer rotates and obtains continuous 360° images of both amplitude and traveltime. Reflection amplitude depends mainly on reflectivity and roughness of the borehole wall. Traveltime depends on diameter of the borehole. The spacing between data pixels is 3 mm vertically and 2.5° or 5° horizontally, depending on acquisition parameters.

The BHTV logging tool includes two accelerometers and three perpendicular magnetometers, for tool orientation. The CRP-3 accelerometer logs indicated that borehole deviation was minor, less than 2.5° from vertical (Cape Roberts Science Team, 2000). The two horizontal magnetometers provide a continuous record of tool orientation with respect to magnetic north, so that all images can be converted from tool coordinates to magnetic north. We converted the images from magnetic north to true North coordinates, using measurements of local deviation based on an on-ice reference magnetometer (Jarrard, Moos, Wilson, Bückner & Paulsen, this volume). The reference magnetometer indicated a local deviation of $147\text{--}148^\circ$, consistent with the International Geomagnetic Reference Field value. The reference magnetometer also confirmed that magnetic storms did not significantly affect local deviation.

BHTV logs were run at a logging speed of 1 m/minute for 92% of the CRP-3 borehole; for details, see Cape Roberts Science Team (2000). Two intervals were not logged because borehole conditions were too unstable to risk losing the tool: the upper fault zone (255.1–271.4 mbsf), and the bottom part of the borehole (898.5–939 mbsf), which was blocked by swelling clays in an altered intrusion. Log quality varied from poor to excellent, generally improving with increasing depth. Much of the top half of the BHTV log provided only rare returns from the borehole wall, possibly because of mudcake. It was usually possible, however, to identify enough features (*i.e.*, fractures, bedding, and clasts) in this upper log to reorientate cores. In the bottom half of the log, these features were much more common and the accuracy of reorientations increased accordingly.

The amplitude images were most useful for identification of geologic features such as fractures, bedding, and clasts. The CRP-3 traveltime logs did not provide reliable measurements of borehole diameter, because of a combination of cycle skipping and poor calibration by the tool manufacturer, Antares®. They occasionally provided useful images of borehole features, particularly open fractures and clasts, but these features generally were imaged as well or better by the amplitude log. Accurate measurement of borehole diameter is required for determination of dip magnitudes, both for bedding and fractures. We assumed a uniform diameter of 102 mm for HQ borehole and 80 mm for NQ borehole, based on dipmeter measurements of borehole diameter (Cape Roberts Science Team, 2000; Bückner, Jarrard, Niessen, and Wonik, this volume).

The CRP-3 BHTV logs, like other CRP-3 well logs, exhibited up to 2.5 m of depth shift compared to coring depths, caused mainly by stretch of the logging cable. This shift varied both between and within logging runs. We corrected the BHTV data to minimize depth shifts, based on identification of 337 correlative features on the core logs (Cape Roberts

Science Team, 2000) and BHTV images. Optimum depth shift was calculated for each of 11 intervals of BHTV log. The final shifted logs have residual depth shifts that are everywhere less than 10 cm, which is satisfactory for reliable correlation of features between core images and BHTV images.

IMAGE MATCHING PROCEDURE

Both stitched-core and BHTV images were first displayed as unwrapped, 0-360° azimuth images. An entire stitched-core image, 5-30 m in length, can be converted from relative azimuth to true North coordinates with a single rotation. The magnitude of this rotation was determined by subjective visual identification of correlative features on the stitched-core and BHTV images. We used three types of features: fractures, bedding, and clasts. Before picking feature azimuths, however, we first identified and quantified depth shifts between stitched-core and BHTV images. These shifts were nearly always less than 10 cm, but even minor unrecognized depth shifts can lead to rare spurious correlation of features.

Feature orientations can be picked in WellCAD® in two ways: single-point and sinusoid. For example, the azimuth of a bed or fracture top or bottom can be picked by just moving a cursor to a single point. The same procedure can be used to determine the orientation of the top, bottom, edge, or center of a clast. Planar features such as most beds and fractures and some large clasts form a sinusoidal shape on these images. Their azimuths can be picked with greater accuracy by fitting a sinusoid to the feature outline; manual sinusoid picking is rapid and easily revised in WellCAD®. One can pick top or bottom or center azimuth of any feature, as long as exactly the same portion of the feature is picked on stitched-core and BHTV images. The difference between azimuths on core and BHTV images is used to reorientate core, by rotating the core to minimize such differences.

For core reorientation, fractures, bedding, and clasts have different advantages and disadvantages. Fractures are generally steep enough and planar enough that their orientations can be picked with an accuracy of $\pm 3^\circ$ on both stitched-core and BHTV images, but many intervals of BHTV have few or no obvious fractures. Because bedding dips are usually shallower ($\sim 10\text{-}30^\circ$) than fracture dips ($\sim 40\text{-}70^\circ$), down-dip azimuths of individual beds have lower accuracies: $\pm 30^\circ$ for $\sim 10^\circ$ dips and $\pm 10^\circ$ for 30° dips on BHTV images, and better on core images. Consequently, we used shallow bedding dips for core reorientation only when several adjacent beds were identifiable. Large clasts have virtually the same shape on both stitched-core and BHTV images, but this generalization does not necessarily hold for small (< 5 cm) clasts, because of the 2-cm drilled-out zone between the outer-core surface and borehole wall. Consequently, individual clasts can have azimuths that

truly differ by $\pm 20^\circ$ between core and borehole wall. A strong advantage of clasts, particularly in the top half of the borehole, is that their reflectivity is so different from surrounding sediments that they are often the only type of geologic feature that can be confidently identified in the BHTV images.

Correction of the stitched-core images to true North was undertaken in two steps. First, while displaying side-by-side core and BHTV images, paired stitched-core and BHTV azimuths were tabulated using single-point (rather than sinusoid) approximate ($\pm 10^\circ$) picks. Differences between stitched-core and BHTV azimuths were averaged to determine a single, first-order correction which was then applied to the stitched-core image. This correction, which generally was accurate to $\pm 15^\circ$, permitted more confident matching of features during the second-order, more accurate phase of reorientation. This second phase involved determination and tabulation of both single-point and sinusoid-picked azimuths, along with depths and types of features. Differences between stitched-core and BHTV azimuths were plotted *vs.* depth for each stitched core, and this plot was examined to identify and exclude any strongly inconsistent picks, and to look for any systematic down-core changes that required further correction. If no systematic changes were detected, all measurements of stitched-core minus BHTV azimuth were used to calculate a single average second-order correction for the stitched-core interval. Figure 1 shows a 0.6 m interval of core and BHTV images after second-order correction,

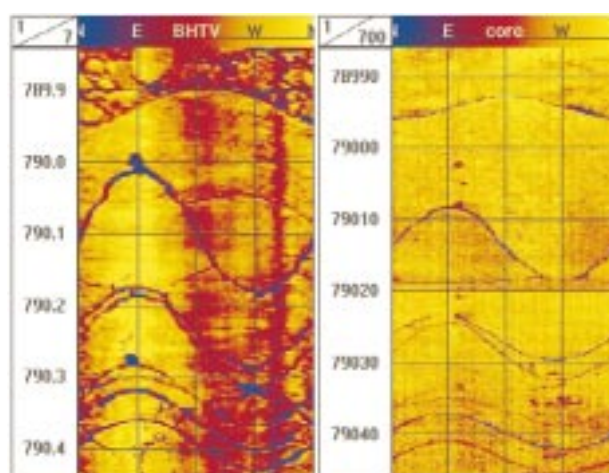


Fig. 1 - Example of a whole-core image (right) that has been reorientated to North by matching feature orientations to those seen on an orientated borehole televiwer image (left). These false-color images are for a 0.6 m interval at the top of a doleritic breccia unit. Most of the image is a single fractured clast; the top of the clast is evident at 789.93 mbsf on the BHTV image and 78995 cm bsf on the core image. Planar features such as the abundant fractures appear as sinusoids on each unwrapped (N-E-S-W-N) image. The sinusoids have higher peak-to-trough amplitudes on the BHTV image than on the whole-core image because the former is larger diameter.

illustrating how a suite of correlative fractures and clast tops provides an unambiguous orientation for this segment of core (as well as for the adjacent 22.9 m of stitched core).

We looked for and sometimes detected two types of systematic down-core changes: drifts and breaks. Sudden breaks, or offsets, of core-BHTV correction angle were identified in about one-fourth of the stitched-core intervals. These breaks indicate a previously undetected rotation between two portions of stitched core, caused by a mismatch of adjacent core segments. Nearly all of the segment matches used within a stitched-core interval are unambiguous and are so noted during initial scribing and later stitching, but a few are less reliable. Whenever our core-BHTV feature matching detected a core break, we checked original notes and core images to identify the precise depth of the break. We then reorientated the intervals above and below the break separately, based on core-BHTV azimuth picks for each interval.

Gradual drifts of core-BHTV correction azimuth appear to be present within most stitched-core intervals. Clockwise (looking down-core) drifts predominate, but counterclockwise drifts also are observed. Most detected drifts total $<20^\circ$ from top to bottom of a stitched-core interval, corresponding to azimuthal drifts of 1-5° per meter. The cause of these small drifts is uncertain. Slight misalignment within the Corescan® equipment can impart gradual rotations of the image, so the instrument was aligned at the

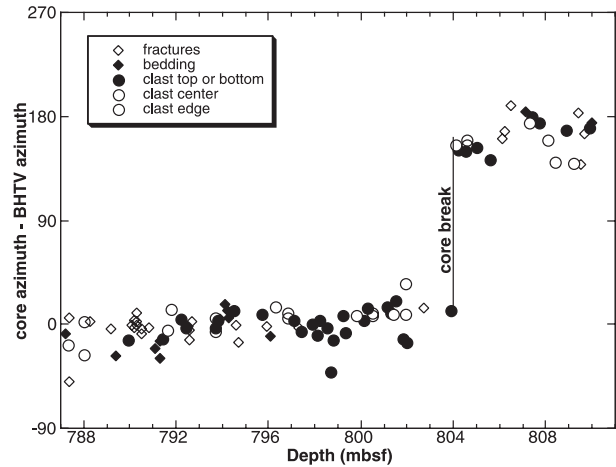


Fig. 2 - Azimuth differences between features on core and borehole televiewer images, after first-order correction. Note consistency of results for different feature types. Also note the previously undetected core break at 804 mbsf.

start of the field season. Because these drifts are too small and imprecisely known to permit accurate removal, we did not apply any within-interval drift corrections.

Table 1 lists the stitched-core intervals that we have reorientated, along with statistics for determinations of core-BHTV correction angle: number of feature matches per core interval, mean reorientation angle (*i.e.*, angle between top of the red

Tab. 1 - Core intervals that have been stitched and reorientated to North.

top depth (mbsf)	bottom depth (mbsf)	#points	reorient. angle stitched image vs. N	std. dev.	95% conf.
204.47	234.47	26	98	17.6	12.8
404.20	413.53	16	308	16.1	8.6
451.08	~460.7	16	250	19.8	10.6
~460.7	463.07	4	86	7.7	12.3
538.72	562.60	31	115	15.3	5.6
574.95	579.48	12	129	22.4	14.2
579.48	588.26	16	303	14.1	7.5
610.48	634.95	29	311	15.3	5.8
640.30	~664.2	19	178	13.2	6.4
~664.2	666.18	6	146	13.5	14.1
693.54	706.59	26	32	11.3	4.6
707.96	723.61	20	294	10.6	5.0
787.03	804.00	72	185	11.6	2.7
804.00	810.48	23	347	15.0	6.5
816.48	821.90	30	188	10.5	3.9
822.13	826.48	30	101	9.5	3.5
826.48	831.48	21	283	7.4	3.4
864.19	866.30	8	56	8.6	7.2
866.30	873.52	15	-1	10.8	6.0
873.60	876.20	11	127	7.6	5.1
876.65	880.44	14	19	11.4	6.6
894.48	904.25	16	262	8.6	4.6

scribe and North), standard deviation, and 95% confidence limits for this mean. Figure 2 provides an example suite of core-BHTV azimuth picks for the interval 787.0-810.5 mbsf. Because this interval has more picks (95 total) than any of the other intervals, it best displays the relative accuracies of different types of picks (fractures, beds, and clasts). All three types are clearly useful and yield concordant results. This interval also exhibits a 150° core break at 804 mbsf, and a subtle clockwise drift of 1°/m.

FRACTURE REORIENTATION PROCEDURE

All fractures within intervals of orientated stitched core were reorientated to North by adding three rotation angles: (1) fracture orientation with respect to red scribe (measured in the field); (2) position of the red scribe on the raw stitched-core image (tabulated during stitching); and (3) rotation angle to rotate the raw stitched-core image to North (determined by matching corresponding features on stitched-core and BHTV images).

RESULTS

The overall core recovery rate for CRP-3 was 97%, and 85% of the whole core was of sufficient integrity for whole-core scanning (Cape Roberts Science Team, 2000). Confident fitting of adjacent core segments is possible for continuous intervals ranging from <10 cm to 30 m in length. Of these potentially stitchable intervals, we selected 17 intervals, 2.4-30.0 m long, for stitching and reorientating via the core-BHTV image matching procedure described above (Tab. 1). A total of 231.3 m, or 25% of the cored interval, was reorientated. We did not reorientate all cores, because the process is labor intensive (~1-2 m per hour) and many intervals have few or no features that can be matched.

Reliability of core orientations can be gauged in two ways: by estimating errors associated with each step of the reorientation process, and by comparing azimuths of feature sets within reorientated cores to those within independent datasets.

The BHTV logs which are used as a ground-truth for core reorientation probably have an azimuth accuracy of $\pm 2^\circ$ for the internal magnetometers (calibrated by Antares®) and $\pm 2^\circ$ for local deviation (measured by our on-ice reference magnetometer). Jarrard, Bückner, Wilson, & Paulsen (this volume) confirm the reliability of the BHTV orientations by comparing average structural dip azimuth for the shelf interval 100-789 mbsf based on BHTV (N66°E), dipmeter (N65°E), and regional seismic reflection profiles (N71°E). However, systematic azimuthal errors of $< 5^\circ$ probably are not resolvable. Based solely on number and standard deviation of core-BHTV azimuth matches for each stitched-core interval, 95% confidence limits for each correction can be calculated (Tab. 1). These confidence limits assume random errors and no undetected core breaks. Third-order drifts of $< 20^\circ$ probably occur within some intervals, not biasing interval-average results but

biasing data from the top and bottom of the interval. Within individual stitched-core intervals, the red-scribe line may drift or jump by 100° or more, but such changes do not imply corresponding orientation errors because the core stitching is much more reliable and accurate than the red scribing. Fracture orientations and palaeomagnetic samples are originally measured with respect to the red scribe with an accuracy of $\pm 10^\circ$, and later picking of red-scribe orientation on the stitched-core images has an accuracy of $\pm 2^\circ$. Combining variances, we estimate that orientation uncertainty is $\pm 10^\circ$ for entire stitched-core intervals, and $\pm 15^\circ$ for individual features such as a single fracture or palaeomagnetic sample.

Figures 3 and 4 provide comparisons of bedding and fractures within reorientated cores to those within nearly independent datasets. The latter are not completely independent, because the orientation process uses a combination of bedding, fracture, and clast azimuth matches, but we have invariably found that the three types of matches are consistent.

Figure 3 shows mean bedding dip directions for five intervals of Beacon sandstone (Jarrard, Bückner, Wilson, & Paulsen, this volume). Bedding orientations were separately picked and averaged from reorientated stitched-core images and orientated BHTV images. For all five intervals, cores and BHTV indicate similar dip azimuths and similar dip magnitudes; 95% confidence limits, not shown, detect no significant differences between core and BHTV dip azimuths from the same interval. Some intervals have significantly different dip directions than others, probably because of brecciation and associated structural tilting, and these differences are reflected by

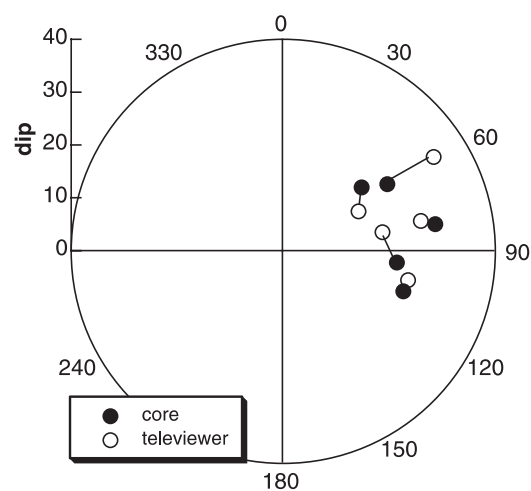


Fig. 3 - Average directions (azimuth and dip) of bedding dip for five reorientated-core intervals of Beacon sandstone (Jarrard, Bückner, Wilson, & Paulsen, this volume), shown as poles to bedding on a zoomed equal area projection (outer circle is 40° dip, not 90°). Note similarity of results from reorientated core images (solid circles) to those from borehole televiewer (open circles) from the same interval (line joining pair of circles).

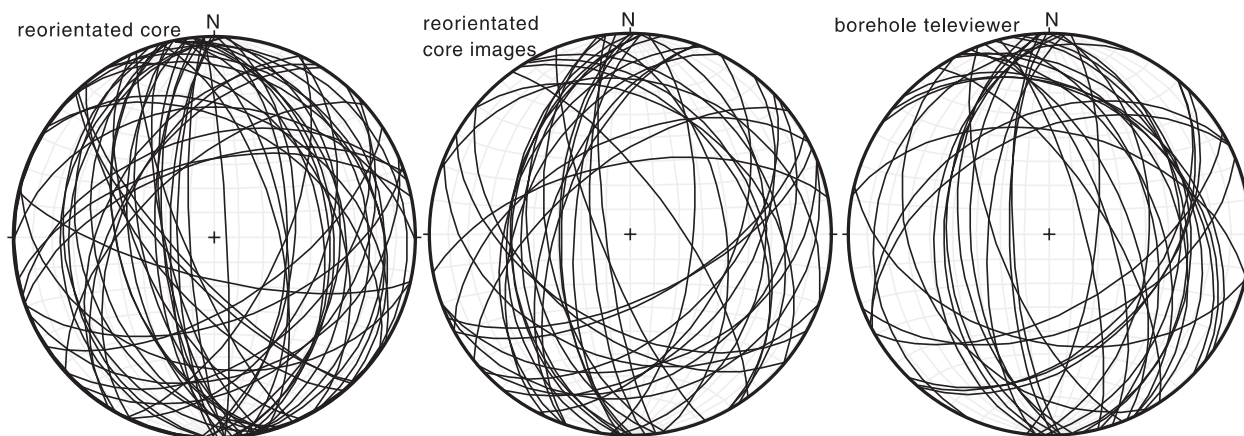


Fig. 4 - Lower-hemisphere equal area projections of fracture orientations within the highly fractured interval 787-804 mbsf (Wilson & Paulsen, this volume). Left: fractures measured on reorientated core. Center: fractures picked on reorientated whole-core images. Right: fractures picked on borehole televiewer images.

similar offsets of both core-based and BHTV-based dip directions.

The deepest fault zone in CRP-3 core is at 790-802 mbsf, within a doleritic breccia. We have been able to stitch and reorientate this entire interval. Figure 4 compares fracture orientations within reorientated core, reorientated stitched-core images, and BHTV images. The three datasets are quite consistent in indicating two fracture sets: steep dips to the west and shallow dips to the ENE. This agreement provides further confirmation of the overall accuracy of the core orientation process.

The reliability of the core reorientation method can be tested by conducting rotation cluster tests on natural fractures found within the core (e.g., Hailwood & Ding, 1995). Fractures should show an improved clustering upon rotation back to *in situ* orientations because they typically form with systematic orientations with respect to a regional stress field (e.g., Kulander et al., 1990). Wilson & Paulsen (this volume) determine fracture orientations for all measured fractures within intervals that have been reorientated to-date. Raw directions are, as expected, virtually random, whereas reorientated fractures exhibit a strong NNE clustering of strikes, thereby demonstrating that the core reorientation process is successful.

The core reorientations of this study provide a framework for several other types of CRP-3 core analysis. The palaeomagnetic results of Florindo et al. (this volume) can provide pole positions rather than just palaeolatitudes. Core fracture patterns are determined by Wilson & Paulsen (this volume), and core bedding patterns are documented by Jarrard, Bückler et al. (this volume).

ACKNOWLEDGEMENTS - This research was supported by the National Science Foundation (OPP-9527319 and OPP-9517394). We sincerely thank C.J. Bückler for BHTV logging and S. Judge for core scanning; their efforts laid the foundation for this project. We thank B. Luyendyk and J. Kück for constructive reviews.

REFERENCES

- Cape Roberts Science Team, 2000. Studies from the Cape Roberts Project, Ross Sea, Antarctica, Initial Report on CRP-3. *Terra Antarctica*, **7**, 1-209.
- Florindo F., Wilson G.S., Roberts A.P., Sagnotti L. & Verosub K.L., 2001. Magnetostratigraphy of late Eocene - early Oligocene strata from the CRP-3 core, Victoria Land Basin, Antarctica. This volume.
- Hailwood E.A. & Ding F., 1995. Palaeomagnetic reorientation of cores and the magnetic fabric of hydrocarbon reservoir sands. In: Turner P. & Turner A. (eds.), *Palaeomagnetic Applications in Hydrocarbon Exploration and Production*, Geol. Soc. Special Pub., **98**, 245-258.
- Jarrard R.D., Bückler C.J., Wilson T.J. & Paulsen T., 2001. Bedding dips from the CRP-3 drillhole, Victoria Land Basin, Antarctica. This volume.
- Kulander B.R., Dean S.L. & Ward B.J. Jr., 1990. *Fractured Core Analysis: Interpretation, Logging, and Use of Natural and Induced Fractures in Core*. Am. Assoc. Petrol. Geol. Methods in Explor. Series, **8**, 88 pp.
- Moos D., Jarrard R.D., Paulsen T.S., Scholz E. & Wilson T.J., 2000. Acoustic borehole televiewer results from CRP-2/2A, Victoria Land Basin, Antarctica. *Terra Antarctica*, **7**, 279-286.
- Paulsen T.S. & Wilson G.S., 1998. Orientation of CRP-1 core. *Terra Antarctica*, **5**, 319-325.
- Paulsen T.S., Wilson T.J., Moos D., Jarrard R.D. & Wilson G.S., 2000. Orientation of CRP-2A core, Victoria Land Basin, Antarctica. *Terra Antarctica*, **7**, 271-278.
- Wilson T.J. & Paulsen T.S., 2001. Fault and fracture patterns in CRP-3 core, Victoria Land Basin, Antarctica. This volume.
- Zemanek J., Glenn E.E., Norton L.J. & Caldwell R.L., 1970. Formation evaluation by inspection with the borehole televiewer. *Geophysics*, **35**, 254-269.